0026-895X/08/7305-1434–1443$20.00
MOLECULAR PHARMACOLOGY
Copyright © 2008 The American Society for Pharmacology and Experimental Therapeutics
Mol Pharmacol 73:1434–1443, 2008

Vol. 73, No. 5
42689/3334040
Printed in U.S.A.

In Vivo Imaging Reveals Selective Peroxisome Proliferator Activated Receptor Modulator Activity of the Synthetic Ligand 3-(1-(4-Chlorobenzyl)-3-*t*-butylthio-5-isopropylindol-2-yl)-2,2-dimethylpropanoic acid (MK-886)

Andrea Biserni, Fabio Giannessi, Anna Floriana Sciarroni, Ferdinando Maria Milazzo, Adriana Maggi, and Paolo Ciana

Department of Pharmacological Sciences, Center of Excellence on Neurodegenerative Diseases, University of Milan, Milan, Italy (A.B., P.C., A.M.); Transgenic Operative Products s.r.l., Lodi, Italy (A.B.); and Department of Endocrinology and Metabolism, Sigma-Tau Industrie Farmaceutiche Riunite S.p.A., Pomezia, Italy (F.G., A.F.S., F.M.M.)

Received October 15, 2007; accepted February 21, 2008

ABSTRACT

We report here the finding of a new pharmacological activity of a well known antagonist of peroxisome proliferator-activated receptors (PPARs). PPARs belong to the family of nuclear receptors playing a relevant role in mammalian physiology and are currently believed to represent a major target for the development of innovative drugs for metabolic and inflammatory diseases. In the present study, the application of reporter animal technology was instrumental to obtain the global pharmacological profiling indispensable to unraveling 3-(1-(4-chlorobenzyl)-3-*t*-butylthio-5-isopropylindol-2-yl)-2,2-dimethylpropanoic acid (MK-886)-selective PPAR modulator (SPPARM) activity not underlined by previous traditional, cell-based studies. The results of this study, demonstrating the usefulness of reporter mice, may open new avenues for the development of innovative drugs for cardiovascular, endocrine, neural, and skeletal systems characterized by limited side effects.

Peroxisome proliferator-activated receptors (PPARs) are nuclear receptors (NRs) closely related to the thyroid hormone and retinoid receptors. The PPAR subfamily of nuclear receptors consists of three different receptors subtypes (PPARα, PPARβ/δ, and PPARγ). Each member of the family heterodimerizes with the retinoid X receptors and binds the responsive elements [peroxisome proliferator-responsive elements (PPREs)] in the promoter region of target genes (Kliewer et al., 1992; Tugwood et al., 1992), where, through interaction with other regulatory proteins, their transcription is modulated. PPARs have been the object of great attention as pharmacological targets because they have been shown to be involved in key physiological functions (lipid and glucose homeostasis, inflammatory processes, and adipogenesis) (Fruchart et al., 1999; Rosen et al., 2000; Kostadinova et al., 2005; Anghel and Wahli, 2007), and their malfunctioning has been associated with major disorders (metabolic syndrome, cardiovascular disease, and diabetes) (Lehmann et al., 1995; Berger and Moller, 2002; Evans et al., 2004; Kota et al., 2005). Moreover, these receptors represent novel potential pharmacological targets for the treatment of rare genetic diseases, such as X-linked adrenoleukodystrophy (Albet et al., 1997; Rampler et al., 2003; Pujol et al., 2004). Thus

The study was supported by Sigma-Tau Industrie Farmaceutiche Riunite S.p.A., Telethon GGP02336, the European Community [Network of Excellence (NoE) Diagnostic Molecular Imaging grant LSHB-CT-2005-512146], NoE European Molecular Imaging Laboratories grant LSHC-CT-2004-503569), Integrated Project Consortium for Research into Nuclear Receptors in Development and Aging grant LSHM-CT-2005-018652, Epigenetic Treatment of Neoplastic Disease grant LSHC-CT-2005-518417, Strep Estrogens and Women Aging grant LSHM-CT-2005-518245, and National Institutes of Health (R01-AG027713-02).

Article, publication date, and citation information can be found at http://molpharm.aspetjournals.org.

doi:10.1124/mol.107.042689.

ABBREVIATIONS: PPAR, peroxisome proliferator-activated receptor; NR, nuclear receptor; PPRE, peroxisome proliferator-responsive element; Wy-14,643, pirinixic acid; MK-886, 3-(1-(4-chlorobenzyl)-3-*t*-butylthio-5-isopropylindol-2-yl)-2,2-dimethylpropanoic acid; ST1929, methyl 2-{4-[2-(4-chlorophenyl)ethoxy]-phenylthio}-2-methylpropanoate; ST2518, [2-{3-[2-(4-chlorophenyl)ethoxy]-phenylthio}-2-methyl propanoic acid; GW501516, (2-methyl-4-(((4-methyl-2-(4-(trifluoromethyl)phenyl)-5-thiazolyl)methyl)thio)phenoxy)-acetic acid; GW9662, 2-chloro-5-nitrobenzanilide; GW1929, (2*S*)-(2-benzoylphenyl)amino-3-[4-[2-(methylpyridin-2-ylamino)ethoxy]phenyl]propionic acid; ERE, estrogen-responsive element; SPPARMs, selective peroxisome proliferator-activated receptor modulators; CMC, carboxymethylcellulose; CCD, charge-coupled device; PCR, polymerase chain reaction; RT, reverse transcriptase; HPLC-MS, high-performance liquid chromatography-mass spectrometry; PRAT, perirenal adipose tissue.

PPARs may represent a new, most relevant target for drug development and have the potential to lead to treatments in areas where there is a major need for novel, efficacious drugs. Because of that, several pharmaceutical companies have engaged in research into the identification of selective ligands for each PPAR subtype, such as the PPARγ agonist thiazolidinediones, developed for the treatment of diabetes, or dyslipidemias. Yet the pharmacological application of the PPAR ligands synthesized so far has been seriously hampered by their major side effects: liver toxicity (Watkins and Whitcomb, 1998; Gale, 2001; Graham et al., 2003; Masubuchi, 2006), negative effects on bone architecture and strength (Rzonca et al., 2004; Lazarenko et al., 2007), tumorigenesis (Berger et al., 2005; Shi et al., 2005), and cardiovascular events (Home et al., 2007; Nissen and Wolski, 2007; Psaty and Furberg, 2007). The difficulties in development of novel drugs targeting PPARs duplicates prior history with other members of the NR family. Indeed, the use of anti-inflammatory drugs targeting glucocorticoid receptors or estrogen receptors in hormonal replacement therapies for postmenopausal women has been limited by the severity of the side effects (Reeves et al., 2006; Conner, 2007; Woolf, 2007). Ubiquitous expression, a hallmark of some of the members of the NR superfamily, represents a major obstacle to overcome for the development of drugs targeting PPARs, estrogen receptors, and glucocorticoid receptors devoid of side effects. On the other hand, the progress in understanding the functions of coregulators and their value in dictating NR tissue specificity of action (McKenna et al., 1999; Robyr et al., 2000; O'Malley, 2007), points to the practicability of projects aiming at finding ligands triggering a tissue-specific activation of NRs to be used in therapy. We believe that more appropriate model systems enabling a global view of drug activity in living organisms would tremendously facilitate the identification of safer therapeutic molecules. Along this line of thought, we generated a reporter mouse (the ERE-*Luc* mouse model) for the global screening of estrogen receptor ligands (Ciana et al., 2001; Maggi et al., 2004) and the strategy devised for this first model was further applied to create a reporter mouse for PPARs (PPRE-*Luc* mouse) (Ciana et al., 2007). The present study was undertaken to verify the suitability of the PPRE-*Luc* mouse for the pharmacological profiling of novel PPAR ligands. By identifying a new SPPARM activity of the well known PPARα antagonist, MK-886, we here provide evidence of the powerfulness of the PPRE-*Luc* mouse model for the identification and characterization of PPAR ligands and show the superiority of this method over the conventional cell-based tests in the prediction of ligand potency and efficacy in vivo.

Materials and Methods

PPAR Ligands. PPARα ligands were obtained as follows: Wy-14,643 was from ChemSyn Laboratories (Kansas City, KS), MK-886 was from BIOMOL International (Plymouth Meeting, PA), and ST1929 was from Sigma-Tau (Pomezia, Italy). PPARβ/σ ligands were obtained as follows: GW501516 was from Axxora Life Sciences Inc. (San Diego, CA). PPARγ ligands were obtained as follows: rosiglitazone and GW9662 were from (Axxora Life Sciences Inc.), GW1929 was from Sigma-Aldrich (St. Louis, MO). Dual PPARα and -γ ligand ST2518 was from Sigma-Tau.

Experimental Animals and Pharmacological Manipulations. Experiments performed in this study were conducted according to the *Guidelines for Care and Use of Experimental Animals*. Use of experimental animal was approved by the Italian Ministry of Research and University and was controlled by the panel of experts of the Department of Pharmacological Sciences, University of Milan. All experiments were carried on with 3- to 5-month-old male PPRE-*Luc* transgenic mice. Mice were kept under a 12-h light/dark regimen. To maximize the reporter response to drug treatments, metabolic activation of PPARs was minimized by feeding mice only during the night (Ciana et al., 2007) for the 48 h preceding the experiment. All the experiments were carried out in the afternoon.

PPARs agonists and antagonists were administered subcutaneously (vehicle used: vegetable oil) or by gavage [vehicle used: water solution of 0.5% carboxymethylcellulose (CMC)]. All ligands were administered 50 and 250 mg/kg s.c. or 50 mg/kg by gavage with the following exceptions: rosiglitazone, 10 and 50 mg/kg s.c. or 5 mg/kg by gavage; GW9662, 25 mg/kg by gavage; and Wy-14,643, 100 mg/kg by gavage. Antagonists were given 30 min before injections of the corresponding agonists. Treatments were performed in the morning (10:00 AM), and photon detection was assayed 6 h later (4:00 PM).

Bioluminescence Reporter Imaging. Mice were visualized with a Night Owl imaging unit (Berthold Technologies, Bad Wildbad, Germany) consisting of a Peltier-cooled charge-coupled device slow-scan camera equipped with a 25-mm, f/0.95 lens. Images were generated by a Night Owl LB981 image processor and transferred via video cable to a peripheral component interconnect frame grabber using WinLight[32] software (Berthold Technologies). For the detection of bioluminescence, mice were anesthetized using an s.c. injection of 50 μl of ketamine-xylazine solution composed of 78% ketamine (Ketavet 50; Intervet, Peschiera Borromeo, Italy), 15% xylazine (2% solution, Rompun; Bayer, Leverkusen, Germany), and 7% water. The mice then received, if not otherwise specified in the text, an i.p. injection of 25 mg/kg D-luciferin (Promega, Madison, WI) 20 min before bioluminescence quantification, to obtain an uniform biodistribution of the substrate. We administered the substrate D-luciferin according to a procedure described previously (Ma et al., 1993; Patrone et al., 1998). Mice were placed in the light-tight chamber and a grayscale photo of the animals was first taken with dimmed light. Photon emission was then integrated over a period of 5 min.

Ex vivo optical imaging assay was performed on dissected tissues. Animals were injected with 25 mg/kg luciferin and killed after 20 min; photon emission from each organ, kept in phosphate-saline buffer, was monitored over a period of 10 min with the Night Owl imaging unit as described above.

Luciferase Enzymatic Assay. For enzymatic assay of luciferase activity, tissues from euthanized mice were dissected and immediately frozen on dry ice. Protein extracts were prepared by homogenization [in a TissueLyser (QIAGEN GmbH, Hilden, Germany)] in 200 μl of 100 mM KPO_4 lysis buffer, pH 7.8, containing 1 mM dithiothreitol, 4 mM EGTA, 4 mM EDTA, and 0.7 mM phenylmethylsulfonyl fluoride), three cycles of freezing-thawing, and 30 min of minifuge centrifugation (Eppendorf AG, Hamburg, Germany) at maximum speed. Supernatants containing luciferase were collected, and protein concentrations were determined by Bradford assay (Bradford, 1976). Luciferase enzymatic activity was measured by a commercial kit (Luciferase assay system; Promega, Madison, WI) according to the supplier's instructions. The light intensity was measured with a luminometer (Veritas; Promega, Madison, WI) over a 10-s time period and expressed as relative light units (RLU) per microgram of protein.

Real-Time PCR Gene Expression Analysis. Real-time PCR experiments were done with total RNAs extracted after tissue homogenization in TRIzol reagent (Invitrogen, Carlsbad, CA) as suggested by the manufacturer's instructions. For the preparation of cDNA, 1 μg of RNA was denatured at 75°C for 5 min in the presence of 1.5 μg of random primers (Promega) in a 15-μl final volume. Deoxynucleotide triphosphate (GE Healthcare) and Moloney murine leukemia virus reverse transcriptase (RT; Promega) were added at

0.5 mM and 8 U/μl final concentration, respectively, in a final volume of 25 μl. The RT reaction was performed at 37°C for 1 h; the enzyme was inactivated at 75°C for 5 min. Control reactions without addition of the RT enzyme were performed for each sample. Real-time PCR experiments were performed using TaqMan technology. The reaction mix for each sample was made up of 5 μl of cDNA (1:25 dilution), 12.5 μl of TaqMan 2× Universal PCR Master Mix No AmpErase UNG (Applied Biosystems, Foster City, CA) and 7.5 μl of primers and probes mix: 300 nM *Abcd2* forward and reward primers (5′-TGGTGGCTTCCAGGCTAAAC-3′, 5′-GGGACCAGTTATCAAGAGATGCA-3′), 200 nM *Abcd2* TaqMan MGB probe 5′-6FAM-TCAAAGTGGAAGAAGGG-MGB-3′; premade TaqMan Gene Expression assays for the endogenous gene *Acox1* (Mm00443579_m1, Applied Biosystems), and as a reference gene assay 18S rRNA VIC-MGB-PDAR (Applied Biosystems). The reaction was carried out according to the manufacturer's protocol using Applied Biosystems 7000 Sequence Detection System device with the following thermal profile: 2 min at 50°C, 10 min 95°C, 40 cycles (15 s at 95°C, 1 min at 60°C), and data were analyzed using the ABI Prism 7000 SDS Software and the $2^{-\Delta\Delta C_t}$ method (Livak and Schmittgen, 2001). The analysis of each sample was repeated six times.

HPLC-MS Analysis of Drug Amount in Tissues. The tissue samples (100 mg) were homogenized in 1.0 ml of ice-cold methanol using a Ultra-Turrax homogenizer (IKA Works Inc. Wilmington, NC). Complete homogenization took 30 s or less. The homogenates were centrifuged for 10 min at 3000*g* at 4 C. The clear supernatant was directly injected onto an HPLC-MS system (Waters Alliance 2695 separation module with automatic injector set at +4°C; Waters Corporation, Milford, MA). Injection volume, 10 μl; column, Symmetry 300TM C4 5 μm, 125 × 4.6 mm; column flow rate, 1 ml/min; mobile phase, 30% water acidified with 0.1% formic acid, 70% methanol acidified with 0.1% formic acid; split after column, 1:8. Waters Micromass ZQ2000 single-quadrupole, operating in positive ion mode set at 324.04 Da, was used as detector [capillary (KV) 4.00; core (V) 33.00].

Statistical Analysis. Statistical analysis was performed with the use of Prism 5.01 (GraphPad Software Inc. San Diego, CA); ANOVA was followed by Bonferroni's test with the only exceptions of data shown in Figs. 2, 5, and 7C, where Student's *t* test was performed.

Results

Reporter Mice: in Vivo Imaging of Reporter Gene Expression. In a luciferase-reporter mouse, in vivo evaluation of the potency of a given ligand to elicit luciferase expression, requires prior study of the diffusion to all organs of the enzyme substrate, D-luciferin, at a concentration sufficient to saturate the reporter enzymatic activity. Therefore, preliminary experiments were carried out to study the kinetics of D-luciferin distribution and to define the dose sufficient to fully activate the luciferase produced in the different tissues. To establish the dynamics of D-luciferin diffusion, PPRE-*Luc* mice were injected i.p. with 79.2 mg/kg D-luciferin and photon emission was quantified, as described under *Materials and Methods*, with a sequence of charge-coupled device (CCD) camera sessions of 5 min each. Figure 1A shows that in chest photon emission was maximal between 10 and 25 min after the i.p. injection and then gradually decreased. The result was consistent with previous observations made in another reporter model, the ERE-*Luc* mouse, where the CCD camera sessions were carried out only for 30 min after i.p. injection of the same dose of D-luciferin (79.2 mg/kg). In the ERE-*Luc* mouse model, we could evaluate photon emission from chest and abdomen: in both areas, maximal luciferase activity was measured between 10 and 15 min, and the emission did not change up to 30 min (Fig. 1B). We concluded that observations made between 20 and 25 min guaranteed the optimal distribution of the substrate to the different tissues. This window of time was therefore selected for future experiments.

Next, we injected PPRE-*Luc* mice with 8.8, 17.6, 26.5, and 79.2 mg/kg D-luciferin. Figure 1C shows that at 20 min after injection, the highest dose of substrate (79.2 mg/kg) determined maximal bioluminescence emission. Once more, the results were superimposable with those of previous studies with ERE-*Luc* mice, where we considered three different doses of luciferin (8.8, 26.5, and 79.2 mg/kg i.p.) (Fig. 1D) and observed maximal bioluminescence with the dose of substrate 79.2 mg/kg. However, because of the toxicity of repeated treatments, particularly when animals were repeatedly anesthetized, the dose of 26.5 mg/kg had to be used, particularly in long-term studies.

Present technology for bioluminescence-based in vivo imaging can be consistently carried out in reporter mice only in two dimensions; thus, the definition of the organ/tissue con-

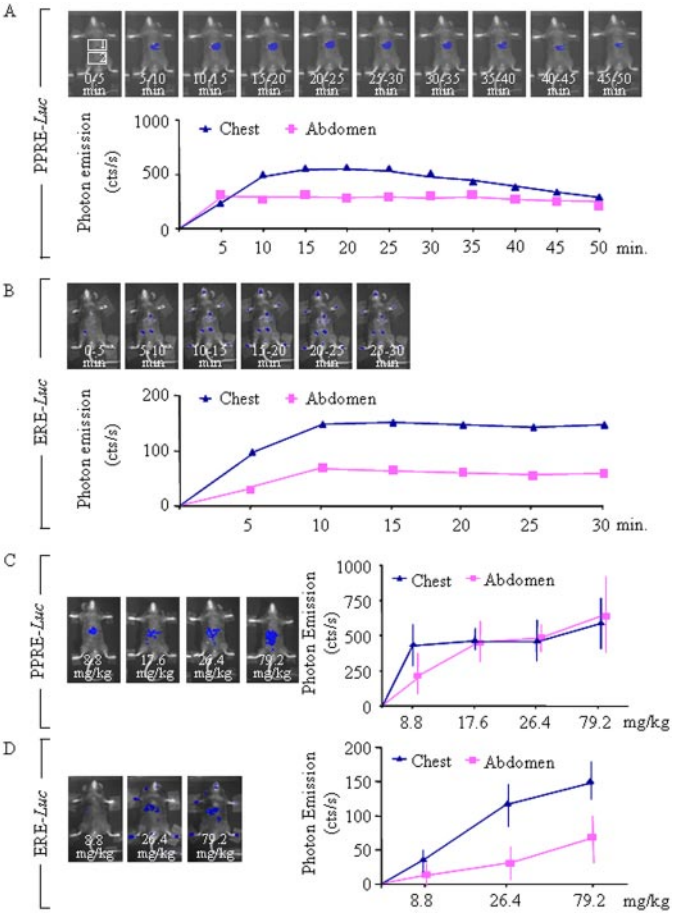

Fig. 1. Biodistribution of luciferase substrate in reporter mice. A and B, optical imaging and photon counting of the luciferase activity of male PPRE-*Luc* and ERE-*Luc* mice i.p. injected with 79.2 mg/kg D-luciferin. Photon emission (cts/s = counts per second) was quantified in selected body areas by a series of 5-min CCD camera acquisitions in each animal. C and D, PPRE-*Luc* and ERE-*Luc* male mice were injected with different doses of D-luciferin (PPRE-*Luc*: 8.8, 17.6, 26.4, and 79.2 mg/kg; ERE-*Luc*: 8.8, 26.4, and 79.2 mg/kg) for 20 min. Photon emission was quantified for 5 min within the indicated body areas. Images show acquisition of a single representative animal, and all data represent the mean ± S.E.M. of acquisitions made in groups of 5 to 10 animals. Photon emission was quantified using an electronic grid as shown in A: grid numbers 1 and 2 delimit the areas named chest and abdomen.

tributing to the photon emission as measured in vivo is limited; furthermore, signaling from the most inner organs is significantly reduced by photon scattering and absorption by the tissues crossed by the photons. Therefore, to better evaluate the homogeneous diffusion of D-luciferin, we carried out a series of ex vivo experiments in which we measured luciferase activity of organs dissected from the mice euthanized at different times after i.p. injection of D-luciferin (26.5 mg/kg). The measurement of the enzyme activity was done first by bioluminescence (Fig. 2, A and B), exposing the dissected organ to the CCD camera, and then the organ was rapidly frozen for the preparation of tissue extracts where luciferase enzymatic activity was measured (Fig. 2C). Luciferase activity, as assessed by enzymatic assay in the tissue extracts, provided results superimposable with CCD-camera quantitative experiments.

The ex vivo experiments were carried out also on animals pretreated with a pharmacological dose (50 mg/kg) of the PPARα agonist Wy-14,643 or vehicle to ensure that the concentration of D-luciferin substrate was adequate for the quantitative measurement of the large amount of luciferase accumulating shortly after stimulation of PPARs. Figure 2 shows the intensity of signaling by isolated organs before and after the pharmacological treatment as measured by bioluminescence (Fig. 2, A and B) or by enzymatic assay (Fig. 2C) in tissue extracts. In Wy-14,643- versus vehicle-treated mice, optical imaging and enzymatic assay showed a significant increase of luciferase activity in liver. High variability in the response was observed in testis and heart, where, as clearly shown by the imaging data, only a minute amount of cells was responsive to the treatment with the PPARα agonist. In brain, luciferase activity was unaffected by the treatment. To verify the reliability of the reporter used in the study, we next measured by real-time PCR the accumulation of *Acyl-CoA oxidase1, palmitoyl* (*Acox1*), a well known PPARα target gene (Stauber et al., 2005) (Fig. 2D). Acox1 mRNA was significantly increased in liver and, similar to what shown with luciferase, this mRNA seemed to be slightly increased in testis and perhaps in heart but not in brain. HPLC-MS measurements of Wy-14,643 content in the various organs showed that the ligand was maximally concentrated in liver and reached heart and, to a lower extent, testis; no brain penetration of the compound was observed (Fig. 2E). These data on drug distribution were consistent with the observed induction of luciferase activity.

***PPRE-Luc* Mouse in Pharmacological Analysis.** To test the ability of PPRE-*Luc* mouse to identify molecules active on all PPAR subtypes, we treated adult male PPRE-*Luc* mice with a series of isoform-specific ligands, such as the PPARα agonist Wy-14,643 (250 mg/kg s.c.), the PPARγ ago-

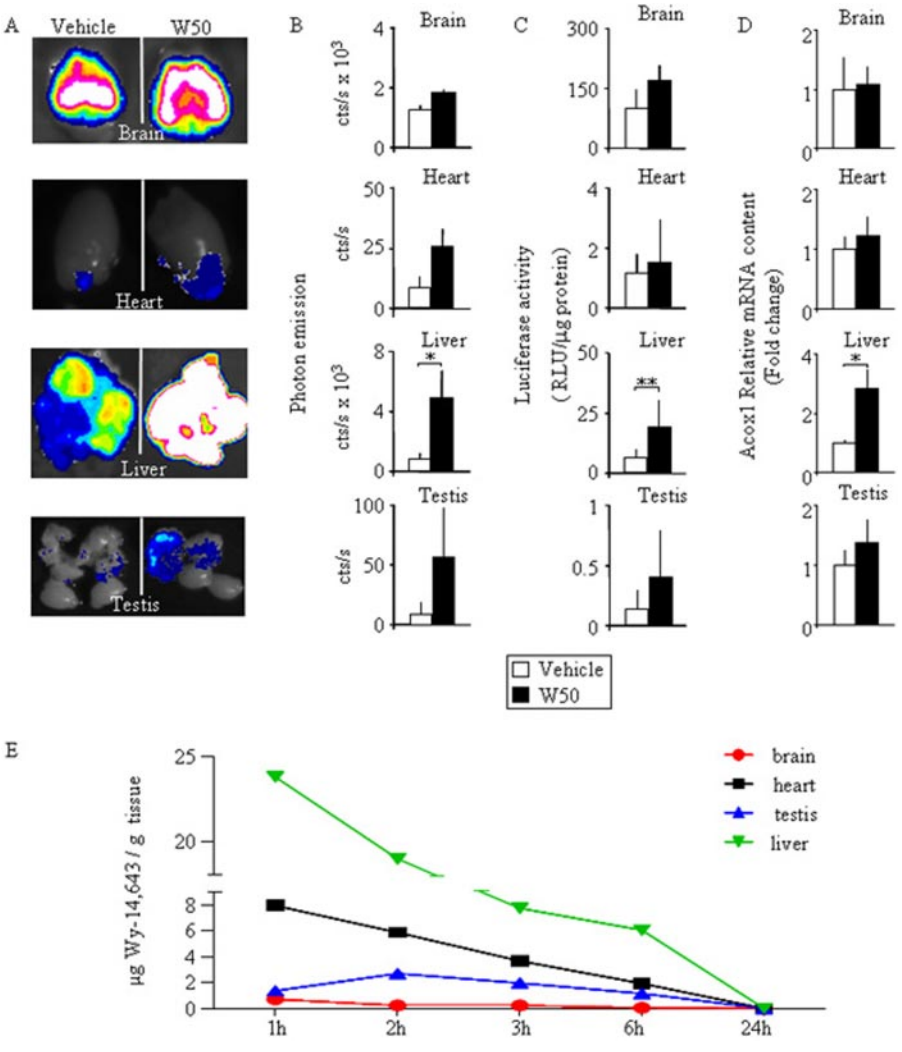

Fig. 2. Ex vivo evaluation of the luciferase activity. PPRE-*Luc* male mice were treated s.c. with 50 mg/kg Wy-14,643 or vehicle and euthanized after 6 h. Organs were rapidly dissected for imaging (A) and photon counting (B) and then frozen for subsequent luciferase analysis by enzymatic assay (C). Luciferase activity was measured by enzymatic assay on protein extracts and expressed as RLUs per microgram of proteins. D, the expression of the endogenous PPARα target gene, *Acox1*, was determined by semiquantitative real-time PCR carried on total mRNA extracted from the indicated tissues. E, measurement of the total amount of Wy-14,643 in brain (red plot), heart (black plot), testis (blue plot), and liver (green plot) was performed by HPLC-MS at 1, 2, 3, 6, and 24 h after Wy-14,643 treatment (50 mg/kg s.c.) and expressed as micrograms of Wy-14,643 per gram of tissue. Bars represent mean ± S.E.M. of five mice. *, $P < 0.05$; **, $P < 0.005$ compared with vehicle treatment. P values were calculated by t test. The experiment was repeated three times.

nists rosiglitazone (50 mg/kg s.c.) and GW1929 (50 mg/kg by gavage), and the PPARβ/δ agonist GW501516 (50 mg/kg by gavage). We also tested two novel compounds (Dell'Uomo et al., 2006): a dual PPARα/PPARγ agonist, ST2518 (250 mg/kg s.c.) and a PPARα-selective agonist ST1929 (250 mg/kg s.c.). Control mice were treated with vehicle (oil for s.c. treatments or 0.5% CMC water solution for gavage treatments). Each mouse was subjected to a CCD camera session at 0, 3, 6, and 24 h after treatment (Fig. 3). Note that the kinetics of the onset of bioluminescence emission were very similar with all compounds tested and were not modified by the route of administration selected for each compound. The highest photon emission was always observed 6 h after treatment and was indistinguishable from controls at 24 h with the only exception of ST2518. This indicates that the activity on PPARs of all ligands, except ST2518, was back to unstimulated levels 24 h after administration, possibly because ST2518 was less readily catabolized.

These kinetics of nuclear receptor activity in response to treatment are in line with previous studies on the ERE-*Luc* reporter mouse by ours (Ciana et al., 2001; Ciana et al., 2003; Maggi et al., 2004) as well as other groups (Lemmen et al., 2004) and are supported by the analysis of the hormonal treatment of endogenous genes (Montani et al., 2008). It is important to underline that the use of firefly luciferase, a protein with a turnover rate of 2 to 3 h, was instrumental to show the cessation of drug action; this would have not been possible with the use of more stable reporters that would have maintained their activity after cessation of receptor activation. The PPARα agonist induced the highest photon emission in chest, as expected on the basis of the high expression of this PPAR receptor subtype in liver; in line with the receptor expression, PPARγ, PPARβ/δ, and PPARα agonists induced luciferase production in abdomen and chest. In fact, it is well known that all PPARs are expressed in the digestive tract. The new compound ST1929 (PPARα agonist) induced maximal luciferase activity in chest at 6 h, but not to a significant extent; we also observed an activity in abdomen that was still high at 24 h.

To better evaluate the extent to which in PPRE-*Luc* mouse the reporter activity reflected the intensity of the signaling on the receptor, we investigated the effect of 6 h treatment with 10 and 50 mg/kg s.c. rosiglitazone (PPARγ) agonist and 50 and 250 mg/kg s.c. of the PPARα agonist Wy-14,643 (Fig. 4). Both in vivo imaging (Fig. 4A) and luciferase enzymatic assay in tissue extracts (Fig. 4B) showed a clear effect of the dosage. Wy-14,643, a PPARα agonist, was active in liver and heart, whereas the PPARγ agonist rosiglitazone was active in liver, intestine, and adipose tissue [perirenal adipose tissue (PRAT); that is, mixed white and brown adipose tissue] but not in heart, a tissue not expressing PPARγ. The use of selective antagonists both for PPARα (250 mg/kg s.c. MK-886) (Kehrer et al., 2001) and PPARγ (50 mg/kg s.c. GW9662) (Leesnitzer et al., 2002) further demonstrated the reliability

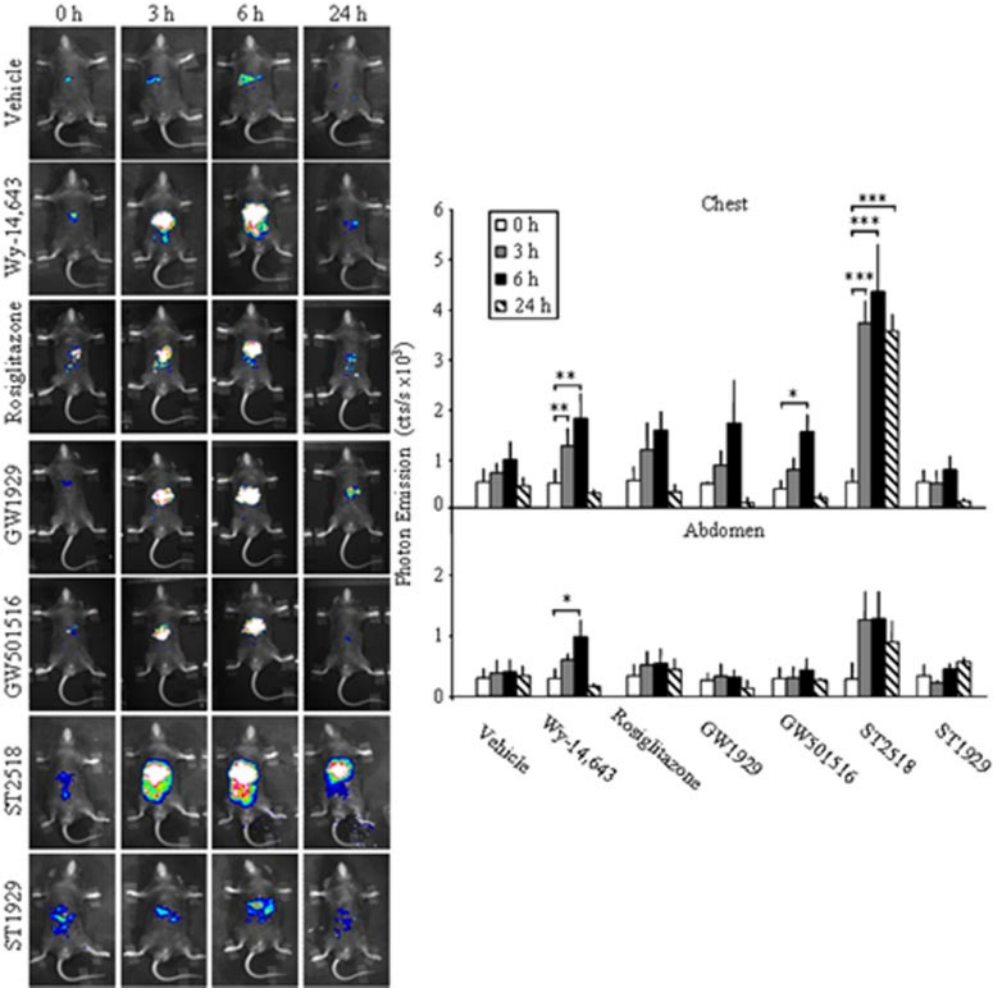

Fig. 3. Time course of the Luciferase activity in PPRE-*Luc* mice after treatment with synthetic PPAR agonists. PPRE-*Luc* mice were treated with Wy-14,643 (PPARα agonist; 250 mg/kg s.c.), rosiglitazone (PPARγ agonist; 50 mg/kg s.c.), GW1929 (PPARγ agonist; 50 mg/kg by gavage), GW501516 (PPARβ/δ agonist; 50 mg/kg by gavage), ST2518 (PPARα and PPARγ dual agonist; 250 mg/kg s.c.), and ST1929 (PPARα agonist; 250 mg/kg s.c.) or vehicle (vegetable oil for s.c. treatments or 0.5% CMC water solution for gavage treatments). Photon emission in chest and abdomen was measured at 0, 3, 6, and 24 h after treatment. On the left, individual animals, each representative of an experimental group, are shown. Bars represent the mean ± S.E.M. of at least five mice. *, $P < 0.05$; **, $P < 0.01$; ***, $P < 0.001$ versus time 0. P values were calculated with ANOVA followed by Bonferroni's test. The experiment was repeated twice.

of the reporter in showing their ability to block the agonist effect on each PPAR subtype. The PPARα antagonist MK-886 significantly reduced luciferase activity in the heart, indicating that PPARα-dependent transcription is constitutively activated in this tissue in untreated condition; the high basal level of transcription seems to preclude further receptor activation after Wy 14,643 administration (Fig. 4B). The antagonist activity of GW9662 in PRAT was further demonstrated on animals subjected to the treatment for a prolonged period of time (Fig. 4C).

Prolonged Treatment with the PPARα-Selective Agonist Wy-14,643 Affects Receptor Signaling. In vivo imaging offers the opportunity to evaluate the effect of a repetitive treatments in the same animal, thus providing a view on the response of the receptor system to the treatment in time. To evaluate the effect of prolonged treatments with a selective PPARα agonist, Wy-14,643 was administered daily at 100 mg/kg/day by gavage for 21 days (Fig. 5A). Most interestingly, during the treatment, the state of transcriptional activity of liver PPARα receptor changed significantly. In the first 5 days of treatment, liver PPARα activity was most stimulated (up to 8–10-fold higher than control mice), but the ability of the agonist to trigger the receptor activity seemed to decrease with time. The results of the in vivo imaging data (Fig. 5A), calculated as the area under the curve (Fig. 5B) during the first 5 days of treatment or during the entire treatment, were confirmed in a subsequent study, in which luciferase activity was measured in liver tissue extracts of animals euthanized after 5 or after 21 days of continuous treatment (Fig. 5C). The negative peaks observed every 6 to 7 days in the graph reporting the daily activity of the PPARs led to speculation on the possibility of a cyclic desensitization of the receptor in response to continuous stimulation.

The study led us to conclude that reporter animals enabled study of the effect of a given drug on its target during time; this ability might provide clues instrumental to optimize dosages and treatment schedules ensuring the maximal effects at the lowest dosage. For instance, the results of our experiment suggest that a discontinuous administration with Wy-14,643 might result in a persistent receptor activity in time, thus providing a more effective treatment with a reduced exposure to the drug.

Screening of PPAR Activity of Novel Molecules. A dose-response study was also carried out in male PPRE-*Luc* mice for the two novel PPAR agonists: ST2518 (shown in cell

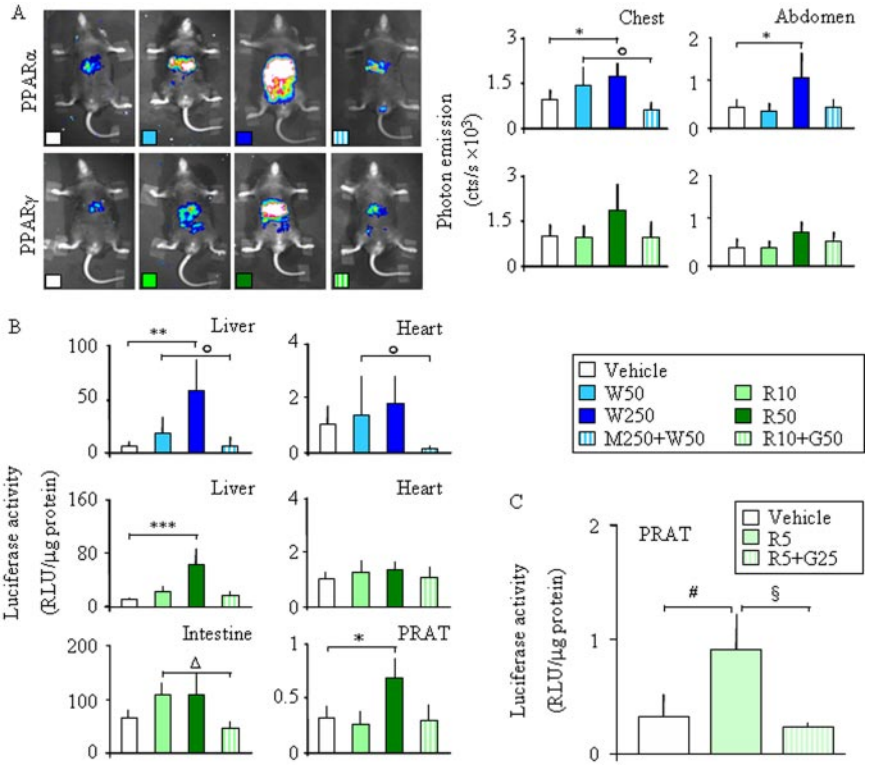

Fig. 4. Modulation of luciferase activity in the PPRE-*Luc* reporter mouse after treatment with selective agonists and antagonists of PPARα and PPARγ. Groups of at least five PPRE-*Luc* male mice were treated s.c. for 6 h with vehicle (vegetable oil, white bars) or the indicated doses of PPARα (Wy-14,643) and PPARγ (rosiglitazone) agonists at the following doses: 50 mg/kg Wy-14,643 (W50, bright blue bars) or 250 mg/kg (W250, dark blue bars); 10 mg/kg rosiglitazone (R10, bright green bars) or 50 mg/kg (R50, dark green bars). Antagonists, 250 mg/kg MK-886 (PPARα) and 50 mg/kg GW9662 (PPARγ), were administered 30 min before s.c. injection of the lower dose of Wy-14,643 (W50+M250, bright blue striped bars) and rosiglitazone (R10+G50, bright green striped bars). A, optical imaging of a representative PPRE-*Luc* mouse (left) and relative quantification of photon emission in chest and abdomen (right). B, ex vivo luciferase activity in liver and heart protein extracts after 6-h treatment with PPARα ligands (top) and in liver, heart, intestine, and PRAT of mice treated with PPARγ ligands (bottom). C, luciferase enzymatic activity on PRAT total protein extracts of mice treated for 10 days by gavage with vehicle (0.5% CMC water solution, white bars), rosiglitazone (5 mg/kg; R5, green bars) and 25 mg/kg GW9662 given 30 min before 5 mg/kg rosiglitazone (R5+G25, green striped bars). Luciferase activity is expressed as RLUs per microgram of proteins. Bars represent the mean ± S.E.M. of five mice. *, $P < 0.01$; **, $P < 0.005$ compared with 6-h vehicle treatment; ○, $P < 0.01$ compared with the W50 treatment; ***, $P < 0.001$ compared with 6-h vehicle treatment. △, $P < 0.05$ compared with 6-h R10 treatment. #, $P < 0.05$ compared with vehicle treatment. §, $P < 0.05$ compared with the R5 treatment; P values were calculated by ANOVA followed by Bonferroni's test. The experiment was repeated twice.

transactivation assay to posses a PPARα and PPARγ dual-agonist activity) and ST1929 (shown to be a PPARα agonist). Two different dosages, 50 and 250 mg/kg s.c., were used. Six hours after treatment with ST2518, in vivo optical imaging analysis revealed a significant luciferase induction in chest and abdomen; no effect was detectable in the testis with both compounds (Fig. 6, A and B). The enzymatic assay (Fig. 6C) confirmed a significant induction of PPARs in liver with ST2518 and a trend to increase with ST1929 treatment. In the heart, the high background in the control group (Ciana et al., 2007), prevented the observation of a clear effect of the agonist: indeed, only a trend to induction of luciferase expression by agonists was measured. The lack of a clear dose-dependent effect on luciferase expression indicated that the lower dose of compound used was sufficient to reach maximum receptor activation. Previous transactivation studies (Dell'Uomo et al., 2006), carried out using the PPARα_{LBD}-GAL4 or PPARγ_{LBD}-GAL4 fusion proteins, showed a comparable efficacy of the two ligands on PPARα (ST1929, methyl ester of the para isomer ST2518: EC_{50}, 31.9 μM; efficacy, 6.8-fold compared with fenofibrate, data not shown; ST2518: EC_{50}, 5.63 μM; efficacy, 7.7-fold compared with fenofibrate). Thus, the in vivo comparison of the ability of ST1929 and ST2518 to transactivate PPARα in the liver of PPRE-*Luc* mice (Fig. 6) shows that the comparable efficacy of the two compounds detected by in vitro studies represent an overestimation of the real potency that ST1929 compound has in the liver of living mice.

***PPRE-Luc* Reporter Mouse Reveals a Remarkable SPPARM Activity in Testis and Lung.** The in vivo imaging analysis of mice treated with PPARα ligands showed that in testis, the selective antagonist MK-886 did not block the agonist Wy-14,643 activity but instead significantly increased it. Furthermore, MK-886 alone induced a highly significant increase of photon emission (Fig. 7A). Additional studies on a wider number of organs of luciferase activity in tissue extracts supported the finding and showed that, when administered alone, MK-886 specifically induces luciferase activity in testis and in lungs (Fig. 7B), and the effect is not additive when MK-886 is administered in combination with Wy-14,643

The results obtained both by in vivo imaging and enzymatic assay were confirmed by the analysis of the expression of endogenous genes by real-time PCR. Figure 7C shows that MK-886 induced *ATP-binding cassette, subfamily D, member 2* (*Abcd2*) and *Acox1* expression in lung; in testis, the changes after the treatment were limited to the Abcd2 mRNA. The lack of activation of *Acox1* might be due to the fact that this

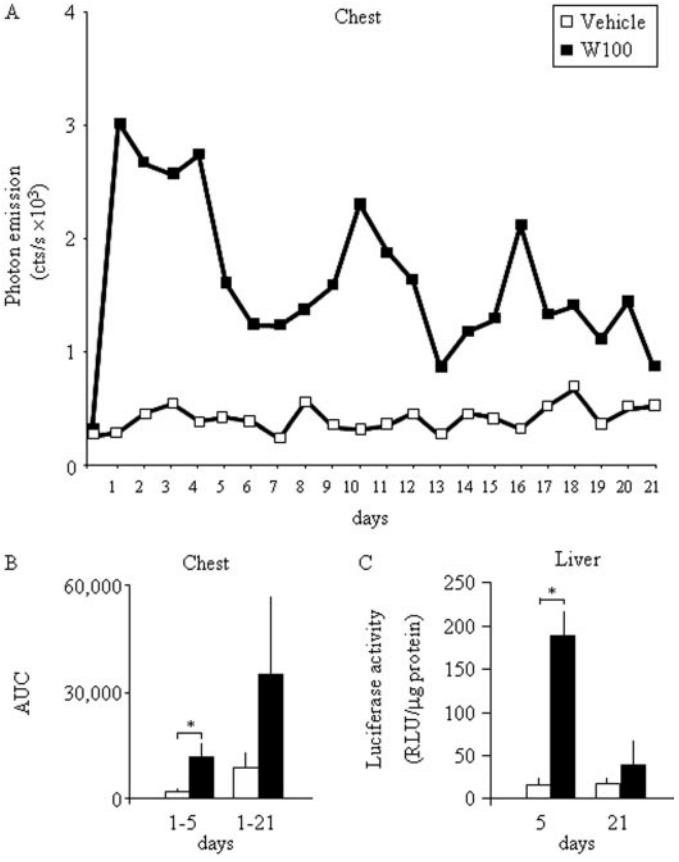

Fig. 5. Imaging of PPARα activation in PPRE-*Luc* reporter mice after repeated administration of Wy-14,643. Groups of five reporter mice were treated daily, for 21 days, with an oral dose of 100 mg/kg Wy-14,643 (■) or vehicle (0.5% CMC water solution, □). A, photon emissions [counts per second (cts/s)] measured in the chest area each day at 4:00 PM (6 h after treatment) were averaged and plotted. B, the graph represents the area under the curve values calculated for the 1 to 5 days and for the entire treatment (1–21 days) on the basis of counts per second measured daily in animals treated with vehicle (open bar) or Wy-14,643 (filled bar). C, luciferase activity was measured in protein extracts from the liver of mice that received the treatment for 5 and 21 days. Bars represent the mean ± S.E.M. of five mice. *, $P < 0.05$ versus vehicle. *P* values were calculated by *t* test. The experiment was repeated twice with superimposable results.

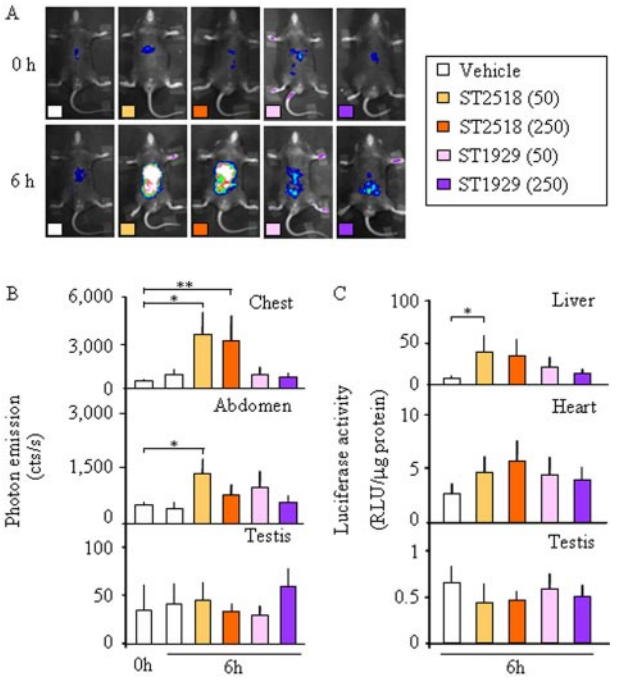

Fig. 6. The profile of PPAR activation in living mice elicited by ST2518 and ST1929, two novel PPAR ligands. Groups of five reporter mice were treated s.c. with 50 or 250 mg/kg ST2518 (bright orange and dark orange labels, respectively), ST1929 (pink and violet labels), or vehicle (white labels). A, optical imaging of one representative PPRE-*Luc* male mouse per group before (0 h) and after 6-h treatment. B, photon emission expressed as counts per second (cts/s), detected by the imaging unit in chest, abdomen, and testis before (0 h) and after 6-h treatment. C, luciferase activity (RLU) measured in protein extracts from liver, heart, and testis after 6-h treatment. Bars represent the mean ± S.E.M. of five mice. *, $P < 0.05$; **, $P < 0.01$ compared with vehicle treatment. *P* values were calculated by ANOVA followed by Bonferroni's test.

gene is not induced by PPARα activation in this organ. Alternatively, the multifactorial control of *Acox1* promoter might limit the analysis of the effect of PPARα ligands, at least in testis. These data indicate that for the pharmacological analysis of PPAR modulators, reporter gene assay in vivo has a higher predictive power than the measurement of endogenous target genes; indeed, reporter synthesis in the PPRE-*Luc* is controlled by a simple promoter where PPAR has a predominant role, whereas the activity of a complex promoter in a natural target gene context is susceptible to a series of inputs that may minimize the contribution of the PPAR activity.

Yet the data on luciferase and endogenous target gene expression are supporting each other in demonstrating a SPPARM activity of MK-886. To the best of our knowledge, this is the first report of a SPPARM activity of this PPAR ligand. It is however important to underline that in addition to its ability to bind PPARα, MK-886 was reported to inhibit 5-lipoxygenase-activating protein and thus to reduce the activity of the lipoxygenase enzymes. This inhibition has the potential to alter the levels of endogenous PPAR ligands; therefore it remains to be established to what extent the PPARα activation observed in testis and lung after MK-866 treatment was due to a local production of a specific ligand or to a direct binding activity of the compound on the receptor leading to a tissue specific recruitment of a coactivator complex.

Discussion

The present study shows the power of reporter mouse technology when applied to pharmacological profiling of drugs active on intracellular receptors. For the first time, the introduction of a surrogate marker offers the possibility to directly titrate the action of a drug on its target in space and time, avoiding extrapolations based on drug distribution parameters. The advantages of the reporter mice over the methods currently in use for preclinical drug development are several and can be summarized as follows: 1) global view of the tissues affected by the treatment that enables a rapid identification of unexpected, potentially undesired effects; 2) unequivocal on-target assessment of dosage and timing necessary to elicit the pharmacological response; 3) possibility to carry out longitudinal studies in single individuals during repeated drug treatment to unravel sites of drug accumulation and activity, or the dynamics of the target response to the treatment (e.g., receptor desensitization or down/up-regulation); and 4) possibility to perform time course studies with limited use of experimental animals.

The present study exemplifies all of the above concepts. First, it demonstrates the importance of in vivo analysis to obtain a global view of the drug effects by describing a novel activity of the PPARα antagonist MK-886. It is well known, in fact, that compounds acting on NR may act as antagonists in one set of cells and as agonists in others. This mixed activity was first described for drugs such as tamoxifen or raloxifene and named Selective Estrogen Receptor Modulators (Katzenellenbogen et al., 1996; Jordan, 2001; Wu et al., 2005; Swaby et al., 2007). The "selective" modulation of NR is due to NR interaction with tissue-specific coregulators that modulate NR ability to induce transcription of target genes (McKenna et al., 1999; Robyr et al., 2000; O'Malley, 2007). The current method to identify NR ligands with mixed agonist/antagonist action is based on the screening of their activity in a series of reporter cells of different tissue origin, often even using synthetic receptors (such as NR_{LBD}-GAL4 fusion protein) unable to correctly interact with coregulators. Our in vivo data show that ligands believed to have similar efficacy in vitro indeed behave quite differently when studied in reporter mice (Fig. 6). This may be ascribed to differential molecular interactions in the target cells or differential adsorption or distribution. In the present study, the limits of in vitro studies are underlined by the fact that they failed to

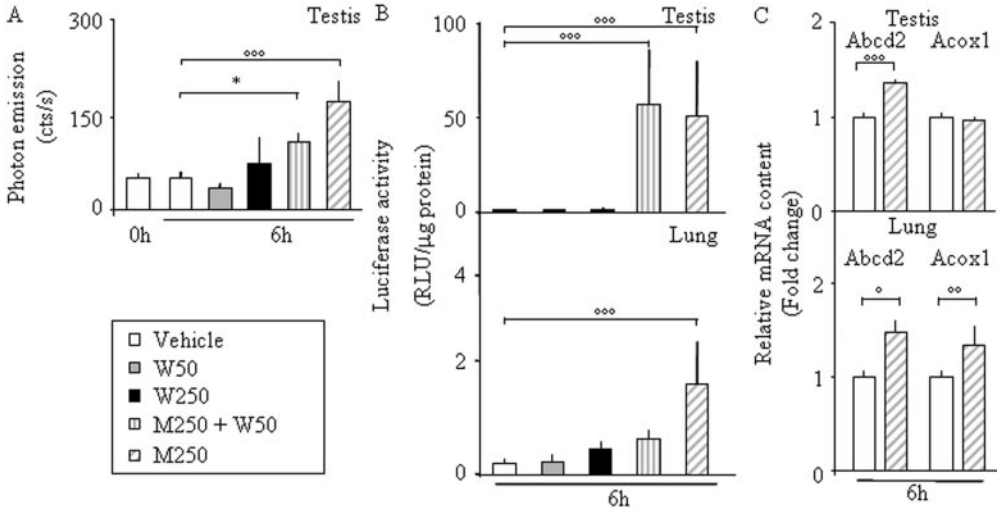

Fig. 7. SPPARM activity of MK-886 in testis and lung revealed by the PPRE-*Luc* reporter mouse. PPRE-*Luc* mice were s.c. injected with vehicle (white bars), 50 (W50, gray bars) and 250 mg/kg (W250, black bars) Wy-14,643, and 250 mg/kg MK-886 administered alone (M250, diagonal striped bars) or 30 min before the 50 mg/kg Wy-14,643 treatment (W50+M250, vertical striped bars). Luciferase activity in testis was measured as photon emission (A) and as enzymatic activity in protein extracts from testis and lung (B). C, the expression of *Abcd2* and *Acox1*, two PPARα target genes, was measured by semiquantitative real-time PCR assay on total mRNA extracted from testis and lung of mice treated for 6 h with vehicle (white bars) and 250 mg/kg MK-886 (M250, diagonal striped bars). Bars represent the mean ± S.E.M. of at least five mice. $*$, $P < 0.05$ versus 6-h vehicle; ○○, $P < 0.005$ versus 6h vehicle; ○○○, $P < 0.001$ versus 6-h vehicle. P values were calculated by ANOVA followed by Bonferroni's test (A and B) or by t test (C). The experiment was repeated twice.

identify the SPPARM activity of MK-886 clearly shown by in vivo imaging using the PPRE-*Luc* mouse model (Fig. 7).

Second, the pharmacological studies here reported illustrate the supremacy of animal reporter systems for the definition of the kinetics of drug action. The observation that all compounds had a peak of activity at 6 h is intriguing; however, due to the high lipophilic profile shared by all compounds, it is possible that all have a very similar kinetics of distribution to the different tissues. On the other hand, the finding that ST2518 differs from all other compounds, maintaining its activity for 24 h, indicates that the reporter system may reveal compounds not readily metabolized or excreted (Fig. 3). In previous studies (Ciana et al., 2003, 2007), we have shown that luciferase activity mirrors the transcriptional activity of the receptor on endogenous target genes. However, the use of endogenous target genes as marker of PPAR activation may lead to conflicting results because of the complexity of endogenous promoters. It is important to stress that the simple PPRE-tk promoter driving luciferase expression in the PPRE-*Luc* model simplifies significantly the analysis of drug activity in the different tissues, eliminating the interference of other transcription regulators, typically acting on the endogenous complex promoters, and leading to ambiguous interpretation on the state of activity of the receptor. A possible drawback for the use of the PPRE-*Luc* reporter mouse is the limited possibility to discriminate which subtype of PPARs is actually contributing to the luciferase expression; however, this problem may be overcome by breeding the model with subtype-specific knockout models or using selective antagonists.

Finally, noninvasive imaging methods facilitate the investigation of drug action when the treatment is continued in time. This is of major interest in developing drugs to be used over the long term; as here shown, the daily examination of the effect of Wy-14,643 administration in individual animals reveals a dynamic response resulting in lowering the drug effect with time (Fig. 5). The analysis of such a response may be crucial for the definition of a timing of compound administration that elicits the highest response at the lowest dosage. In addition, the longitudinal study enables the identification of sites more susceptible to the effect of the drug as a result of local accumulation of the drug or to the absence of physiological protective mechanism of feedback.

Potential limitations of the current in vivo technology are poor high throughput and the two-dimensional imaging. The progress in the imaging field, such as the three-dimensional CCD camera or the development of novel and more powerful reporter proteins for optical imaging (new luciferase mutant protein with a photon emission more shifted in the red spectrum) and for positron emission tomography, will soon overcome present restrictions, yet the use of ex vivo analysis provides a powerful method for the detailed study of the effects of large number of compounds. The reliability of imaging technology in isolated organs is here demonstrated by measuring luciferase enzymatic activity or photon emission in selected organs (Fig. 2). Thus ex vivo imaging could represent a very useful method for the precise and rapid measurement of the time frame and dosage necessary to elicit a pharmacological response or the accessibility of the drug to a given organ (e.g., brain).

In the past 20 years, we have witnessed major changes in drug research programs with a progressive adoption of in silico and cellular approaches driven by the cost-effectiveness of these methods and by the global pressure to limit the use of experimental animals. However, animal engineering by providing novel disease models is giving a new impetus to biomedical research facilitating the understanding of the normal functioning of molecules, cells, organ systems, and whole organisms and the changes induced by different pathologic conditions. The use of reporter systems in disease models will certainly have an invaluable effect for the development and assessment of novel therapies, for the biological characterization of the disease and response to the drug, to titrate drug to disease response in tissues for accurate dosing, and to determine whether the drug modifies the biological disease process or restores a normal process affected by disease with a dramatic improvement in the generation of novel and more efficacious drugs.

Acknowledgments

We thank Cristina Martelli, Clara Meda, Balaji Ramachandran, Monica Rebecchi, and Alessandro Peschechera for their technical assistance. We acknowledge the veterinarian support of Paolo Sparaciari all through the study.

References

Albet S, Causeret C, Bentejac M, Mandel JL, Aubourg P, and Maurice B (1997) Fenofibrate differently alters expression of genes encoding ATP-binding transporter proteins of the peroxisomal membrane. *FEBS Lett* **405:**394–397.
Anghel SI and Wahli W (2007) Fat poetry: a kingdom for PPARgamma. *Cell Res* **17:**486–511.
Berger J and Moller DE (2002) The mechanisms of action of PPARs. *Annu Rev Med* **53:**409–435.
Berger JP, Akiyama TE, and Meinke PT (2005) PPARs: therapeutic targets for metabolic disease. *Trends Pharmacol Sci* **26:**244–251.
Bradford MM (1976) A rapid and sensitive method for the quantitation of microgram quantities of protein utilizing the principle of protein-dye binding. *Anal Biochem* **72:**248–254.
Ciana P, Di Luccio G, Belcredito S, Pollio G, Vegeto E, Tatangelo L, Tiveron C, and Maggi A (2001) Engineering of a mouse for the in vivo profiling of estrogen receptor activity. *Mol Endocrinol* **15:**1104–1113.
Ciana P, Raviscioni M, Mussi P, Vegeto E, Que I, Parker MG, Lowik C, and Maggi A (2003) In vivo imaging of transcriptionally active estrogen receptors. *Nat Med* **9:**82–86.
Ciana P, Biserni A, Tatangelo L, Tiveron C, Sciarroni AF, Ottobrini L, and Maggi A (2007) A novel peroxisome proliferator-activated receptor responsive element-luciferase reporter mouse reveals gender specificity of peroxisome proliferator-activated receptor activity in liver. *Mol Endocrinol* **21:**388–400.
Conner P (2007) Breast response to menopausal hormone therapy–aspects on proliferation, apoptosis and mammographic density. *Ann Med* **39:**28–41.
Dell'Uomo N, Tassoni E, Brunetti T, Pessotto P, Sciarroni AF, Milazzo FM, De Angelis F, Peschechera A, Tinti MO, Carminati P, et al. (2006) 2-{3-[2-(4-chlorophenyl)ethoxy]phenylthio}-2-methylpropanoic acid: a fibrate-like compound with hypolipidemic and antidiabetic activity. *Chem Med Chem* **1:**49–53.
Evans RM, Barish GD, and Wang YX (2004) PPARs and the complex journey to obesity. *Nat Med* **10:**355–361.
Fruchart JC, Duriez P, and Staels B (1999) Peroxisome proliferator-activated receptor-alpha activators regulate genes governing lipoprotein metabolism, vascular inflammation and atherosclerosis. *Curr Opin Lipidol* **10:**245–257.
Gale EA (2001) Lessons from the glitazones: a story of drug development. *Lancet* **357:**1870–1875.
Graham DJ, Green L, Senior JR, and Nourjah P (2003) Troglitazone-induced liver failure: a case study. *Am J Med* **114:**299–306.
Home PD, Pocock SJ, Beck-Nielsen H, Gomis R, Hanefeld M, Jones NP, Komajda M, and McMurray JJ (2007) Rosiglitazone evaluated for cardiovascular outcomes–an interim analysis. *N Engl J Med* **357:**28–38.
Jordan VC (2001) Selective estrogen receptor modulation: a personal perspective. *Cancer Res* **61:**5683–5687.
Katzenellenbogen JA, O'Malley BW, and Katzenellenbogen BS (1996) Tripartite steroid hormone receptor pharmacology: interaction with multiple effector sites as a basis for the cell- and promoter-specific action of these hormones. *Mol Endocrinol* **10:**119–131.
Kehrer JP, Biswal SS, La E, Thuillier P, Datta K, Fischer SM, and Vanden Heuvel JP (2001) Inhibition of peroxisome-proliferator-activated receptor (PPAR)alpha by MK886. *Biochem J* **356:**899–906.
Kliewer SA, Umesono K, Noonan DJ, Heyman RA, and Evans RM (1992) Convergence of 9-cis retinoic acid and peroxisome proliferator signalling pathways through heterodimer formation of their receptors. *Nature* **358:**771–774.
Kostadinova R, Wahli W, and Michalik L (2005) PPARs in diseases: control mechanisms of inflammation. *Curr Med Chem* **12:**2995–3009.
Kota BP, Huang TH, and Roufogalis BD (2005) An overview on biological mechanisms of PPARs. *Pharmacol Res* **51:**85–94.

Lazarenko OP, Rzonca SO, Hogue WR, Swain FL, Suva LJ, and Lecka-Czernik B (2007) Rosiglitazone induces decreases in bone mass and strength that are reminiscent of aged bone. *Endocrinology* **148:**2669–2680.
Leesnitzer LM, Parks DJ, Bledsoe RK, Cobb JE, Collins JL, Consler TG, Davis RG, Hull-Ryde EA, Lenhard JM, Patel L, et al. (2002) Functional consequences of cysteine modification in the ligand binding sites of peroxisome proliferator activated receptors by GW9662. *Biochemistry* **41:**6640–6650.
Lehmann JM, Moore LB, Smith-Oliver TA, Wilkison WO, Willson TM, and Kliewer SA (1995) An antidiabetic thiazolidinedione is a high affinity ligand for peroxisome proliferator-activated receptor gamma (PPAR gamma). *J Biol Chem* **270:**12953–12956.
Lemmen JG, Arends RJ, van Boxtel AL, van der Saag PT, and van der Burg B (2004) Tissue- and time-dependent estrogen receptor activation in estrogen reporter mice. *J Mol Endocrinol* **32:**689–701.
Livak KJ and Schmittgen TD (2001) Analysis of relative gene expression data using real-time quantitative PCR and the 2(-ΔΔCt) method. *Methods* **25:**402–408.
Ma ZQ, Spreafico E, Pollio G, Santagati S, Conti E, Cattaneo E, and Maggi A (1993) Activated estrogen receptor mediates growth arrest and differentiation of a neuroblastoma cell line. *Proc Natl Acad Sci U S A* **90:**3740–3744.
Maggi A, Ottobrini L, Biserni A, Lucignani G, and Ciana P (2004) Techniques: reporter mice—a new way to look at drug action. *Trends Pharmacol Sci* **25:**337–342.
Masubuchi Y (2006) Metabolic and non-metabolic factors determining troglitazone hepatotoxicity: a review. *Drug Metab Pharmacokinet* **21:**347–356.
McKenna NJ, Lanz RB, and O'Malley BW (1999) Nuclear receptor coregulators: cellular and molecular biology. *Endocr Rev* **20:**321–344.
Montani C, Penza M, Jeremic M, Biasiotto G, La Sala G, De Felici M, Ciana P, Maggi A, and Di Lorenzo D (2008) Genistein is an efficient estrogen in the whole body throughout mouse development. *Toxicol Sci* **67:**681–694.
Nissen SE and Wolski K (2007) Effect of rosiglitazone on the risk of myocardial infarction and death from cardiovascular causes. *N Engl J Med* **356:**2457–2471.
O'Malley BW (2007) Coregulators: from whence came these "master genes". *Mol Endocrinol* **21:**1009–1013.
Patrone C, Gianazza E, Santagati S, Agrati P, and Maggi A (1998) Divergent pathways regulate ligand-independent activation of ER alpha in SK-N-BE neuroblastoma and COS-1 renal carcinoma cells. *Mol Endocrinol* **12:**835–841.
Psaty BM and Furberg CD (2007) The record on rosiglitazone and the risk of myocardial infarction. *N Engl J Med* **357:**67–69.
Pujol A, Ferrer I, Camps C, Metzger E, Hindelang C, Callizot N, Ruiz M, Pampols T, Giros M, and Mandel JL (2004) Functional overlap between ABCD1 (ALD) and ABCD2 (ALDR) transporters: a therapeutic target for X-adrenoleukodystrophy. *Hum Mol Genet* **13:**2997–3006.
Rampler H, Weinhofer I, Netik A, Forss-Petter S, Brown PJ, Oplinger JA, Bugaut M, and Berger J (2003) Evaluation of the therapeutic potential of PPARalpha agonists for X-linked adrenoleukodystrophy. *Mol Genet Metab* **80:**398–407.
Reeves GK, Beral V, Green J, Gathani T, and Bull D (2006) Hormonal therapy for menopause and breast-cancer risk by histological type: a cohort study and meta-analysis. *Lancet Oncol* **7:**910–918.
Robyr D, Wolffe AP, and Wahli W (2000) Nuclear hormone receptor coregulators in action: diversity for shared tasks. *Mol Endocrinol* **14:**329–347.
Rosen ED, Walkey CJ, Puigserver P, and Spiegelman BM (2000) Transcriptional regulation of adipogenesis. *Genes Dev* **14:**1293–1307**.**
Rzonca SO, Suva LJ, Gaddy D, Montague DC, and Lecka-Czernik B (2004) Bone is a target for the antidiabetic compound rosiglitazone. *Endocrinology* **145:**401–406.
Shi GQ, Dropinski JF, McKeever BM, Xu S, Becker JW, Berger JP, MacNaul KL, Elbrecht A, Zhou G, Doebber TW, et al. (2005) Design and synthesis of alpha-aryloxyphenylacetic acid derivatives: a novel class of PPARalpha/gamma dual agonists with potent antihyperglycemic and lipid modulating activity. *J Med Chem* **48:**4457–4468.
Stauber AJ, Brown-Borg H, Liu J, Waalkes MP, Laughter A, Staben RA, Coley LC, Swanson C, Voss KA, Kopchick JJ, et al. (2005) Constitutive expression of peroxisome proliferator-activated receptor α-regulated genes in dwarf mice. *Mol Pharmacol* **67:**681–694.
Swaby RF, Sharma CG, and Jordan VC (2007) SERMs for the treatment and prevention of breast cancer. *Rev Endocr Metab Disord* **8:**229–239.
Tugwood JD, Issemann I, Anderson RG, Bundell KR, McPheat WL, and Green S (1992) The mouse peroxisome proliferator activated receptor recognizes a response element in the 5′ flanking sequence of the rat acyl CoA oxidase gene. *EMBO J* **11:**433–439.
Watkins PB and Whitcomb RW (1998) Hepatic dysfunction associated with troglitazone. *N Engl J Med* **338:**916–917.
Woolf AD (2007) An update on glucocorticoid-induced osteoporosis. *Curr Opin Rheumatol* **19:**370–375.
Wu YL, Yang X, Ren Z, McDonnell DP, Norris JD, Willson TM, and Greene GL (2005) Structural basis for an unexpected mode of SERM-mediated ER antagonism. *Mol Cell* **18:**413–424.

Address correspondence to: Adriana Maggi, Center of Excellence on Neurodegenerative Diseases, Department of Pharmacological Sciences, University of Milan, Via Balzaretti 9, 20133 Milan, Italy. E-mail: adriana.maggi@unimi.it